Intensities of backscatter Mössbauer spectra

Z. Mei
Center for Advanced Materials, Lawrence Berkeley Laboratory and Department of Materials Science and Mineral Engineering, University of California, Berkeley, California 94720

B. Fultz
Department of Materials Science, California Institute of Technology, 138-78, Pasadena, California 91125

J. W. Morris, Jr.
Center for Advanced Materials, Lawrence Berkeley Laboratory and Department of Materials Science and Mineral Engineering, University of California, Berkeley, California 94720

(Received 5 January 1988; accepted for publication 26 April 1988)

The intensities of γ-ray and x-ray backscatter Mössbauer spectra of ^{57}Fe nuclei in different matrix materials were studied theoretically and experimentally. A previous analysis by J. J. Bara [Phys. Status Solidi A **58**, 349 (1980)] showed that negative peak intensities occur in backscatter γ-ray spectra when the ^{57}Fe nuclei are in a matrix of light elements. We report a confirmation of this work and offer a simple explanation of the phenomenon. The present paper extends Bara's analysis to the case of conversion x-ray spectra; expressions for the intensity of conversion x-ray spectra as a function of absorber thickness and absorber material parameters are presented. We show that negative peak intensities are expected in conversion x-ray spectra when the ^{57}Fe nuclei are in a matrix of heavy elements.

I. INTRODUCTION

A critical problem in utilizing Mössbauer spectrometry for quantitative measurements is the dependence of spectral intensities on specimen thickness. Thickness correction procedures are well developed for transmission Mössbauer spectra, but less so for backscatter Mössbauer spectra obtained with the experimental geometry shown in Fig. 1(a). Although several early analyses of absorber thickness effects in γ-ray backscatter spectra were attempted,[1–3] a full treatment was not available until recently (Bara and co-worker[4–6]). Some nonintuitive phenomena are predicted by Bara's theory. Unlike the monotonic saturation of the peak height versus absorber thickness for transmission experiments, in ^{57}Fe backscatter experiments the peak height was shown to saturate nonmonotonically with absorber thickness, and in some cases the peak height may saturate to negative values (e.g., Fe in coal[7]), which means "dips" rather than "peaks" are obtained in backscatter spectra. Bara observed negative amplitudes in γ-ray backscatter spectra.[8]

In the present paper we first review Bara's theory and provide a physical description of the nonmonotonic saturation of peak height versus absorber thickness and the origin of negative amplitudes in γ-ray backscatter Mössbauer spectra. We then extend Bara's theory of thickness effects in backscatter spectra to the case of conversion x-ray backscatter spectra. The tendencies towards negative intensities in conversion x-ray and γ-ray backscatter experiments are shown to depend on the density of the absorber matrix in opposite ways. Calculated intensities for absorbers of different thicknesses are then compared to experimental intensities in γ-ray spectra and conversion x-ray backscatter spectra.

II. THEORY

A. Analysis of γ-ray backscatter Mössbauer spectra

For the experimental geometry shown in Fig. 1(a), Bara's theory includes seven contributions to the backscatter γ-ray intensity. Both recoilless and nonrecoilless γ rays from the source are considered. Only the recoilless γ rays can be resonantly absorbed by the ^{57}Fe in the absorber, but like the nonrecoilless γ rays they are also subject to Rayleigh scattering (the scattering of incident γ rays by tightly bound electrons) and Compton scattering (the scattering of incident γ rays by loosely bound electrons). Rayleigh scattering may occur with no loss of γ ray energy so that a γ ray which has undergone Rayleigh scattering may later induce a nuclear resonance. The first five of Bara's seven contributions include the recoilless incident γ rays that are scattered (1) by nuclear resonance recoillessly, (2) by nuclear resonance nonrecoillessly, (3) by Rayleigh scattering recoillessly, (4) by Rayleigh scattering nonrecoillessly, and (5) by Compton scattering nonrecoillessly. The other two contributions include the nonrecoilless incident γ rays that are scattered nonresonantly (6) by Rayleigh scattering, and (7)

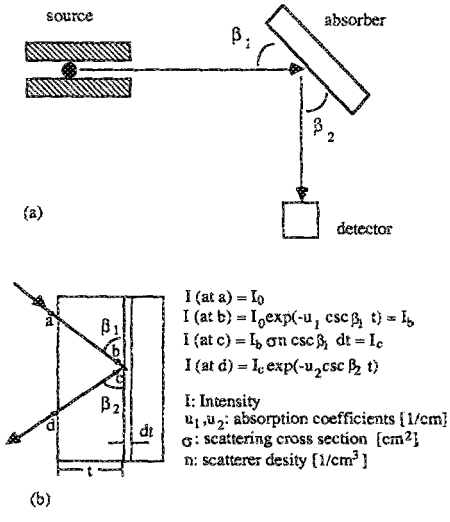

FIG. 1. (a) Backscatter geometry used in analysis. (b) Model used to derive the mathematical expression of backscattered intensity.

 0021-8979/88/172550-06$02.40

by Compton scattering. The mathematical expression for each of the seven contributions as functions of absorber thickness and material parameters can be derived based on the model shown in Fig. 1(b). In addition, the dependence of resonant absorption on incident γ ray energy has to be considered. The final forms of the seven expressions involve complicated integrations. They are given in Ref. 6.

The sum of seven contributions is the total γ-ray intensity N at the detector, and the dependence of N on v, the Doppler velocity, is the Mössbauer spectrum. Unless otherwise stated in this paper we assumed a single-line spectrum with the maximum resonance absorption at $v=0$. It is usually found, and generally accepted, that there will be a peak in backscatter Mössbauer spectra at $v=0$, i.e., $N(0)>N(\infty)$.

In general, the peak height, $N(0)-N(\infty)$, does not increase monotonically with the absorber thickness. As shown in Fig. 2(a), both $N(0)$ and $N(\infty)$ increase monotonically to saturation as the absorber is made thicker. However, $N(0)$ saturates faster than $N(\infty)$ does, because at resonance the incident γ rays are absorbed both resonantly and nonresonantly, while off resonance the incident γ rays are abosrbed only nonresonantly. It is the difference between the saturation distances of $N(0)$ and $N(\infty)$ that causes the nonmonotonic variation of the peak height with the specimen thickness.

Another important parameter in the Mössbauer spectrum is the percentage effect, I_f defined as

$$I_f=\frac{N(0)-N(\infty)}{N(\infty)}=\frac{N(0)}{N(\infty)}-1. \tag{1}$$

It decreases and saturates with absorber thickness starting from a *nonzero* value at zero thickness to a saturated value at infinite thickness, as shown in Fig. 2(b). Although Fig. 2(a) shows that $N(0)$ becomes zero as the thickness decreases to zero, $N(\infty)$ also goes to zero. By L'Hospital's rule applied to $N(0)$ and $N(\infty)$ at zero thickness,

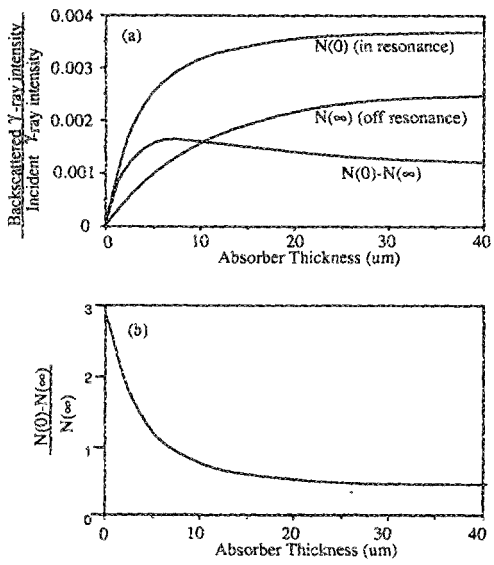

FIG. 2. (a) Numerically calculated γ-ray backscatter Mössbauer spectrum intensity vs stainless steel absorber thickness (Ref. 7). (b) Numerically calculated percentage effect of a γ-ray backscatter Mössbauer spectrum vs stainless-steel absorber thickness.

$$\frac{N(0)}{N(\infty)}=\frac{dN(0)}{dt}\Big/\frac{dN(\infty)}{dt}$$
$$=\frac{\frac{1}{2}f_0U_r/(1+\alpha)+U_R+U_C}{U_R+U_C}, \tag{2}$$

which is the slope of the $N(0)$ curve at zero thickness divided by the slope of the $N(\infty)$ curve at zero thickness, where f_0 is the recoilless fraction of incident γ rays, α is the internal conversion coefficient, U_r is the nuclear resonant absorption coefficient ($U_r=f_1pn\sigma_0$), p is the abundance of the resonant isotope, σ_0 is the nuclear resonance cross section, n is the number of ^{57}Fe nuclei per cm^3, and U_R and U_C are nonresonant Rayleigh and Compton absorption coefficients.

Perhaps the most interesting prediction is that in some cases the peak height may be negative, i.e., "dips" rather than "peaks" are obtained in backscatter γ-ray spectra. The condition for negative intensities is now developed for an infinitely thick absorber, a case that includes many practical situations. Solving the integral expressions for the seven contributions[6] for infinite thickness, adding up to get the total intensity N, and calculating N for $\Delta=0$ and $\Delta=\infty$, respectively, we obtain

$$N(0)-N(\infty)\propto\frac{f_1U_r}{(1+\alpha)X_r(X_r+1)}+\frac{(1-f_1)U_r}{(1+\alpha)X_n(X_n+1)}+\frac{f_RU_R}{X_r}+\frac{(1-f_R)U_R}{X_n}+\frac{U_C}{X_n}-U_R-U_C, \tag{3}$$

where f_1 is the recoilless fraction of the absorber, f_R is the recoilless for Rayleigh scattering. X_r is equal to the square root of $1+U_r/U$, U is the total nonresonant absorption coefficient ($U=U_R+U_C+U_p$, where U_p is the photoelectronic absorption coefficient), X_n is equal to square root of $1+U_r\csc\beta_1/U(\csc\beta_1+\csc\beta_2)$, and β_1 and β_2 are defined in Fig. 1.

Rewriting Eq. (3), we have

$$N(0)-N(\infty)\propto\frac{U_r}{(1+\alpha)X_r(X_r+1)}+\frac{(1-f_1)U_r}{(1+\alpha)}\times\left(\frac{1}{X_n(X_n+1)}-\frac{1}{X_r(X_r+1)}\right)+\frac{U_R+U_C}{X_r}-U_R-U_C+(1-f_R)\times U_R\left(\frac{1}{X_n}-\frac{1}{X_r}\right)+U_C\left(\frac{1}{X_n}-\frac{1}{X_r}\right). \tag{4}$$

It is possible for Eq. (4) to be less than zero, so negative intensities in γ-ray backscatter spectra can occur. An approximation leads to an intuitive interpretation. Assume that

$$\frac{1}{X_n(X_n+1)}-\frac{1}{(X_r(X_r+1)}\ll\frac{1}{X_r(X_r+1)}, \tag{5}$$

$$\frac{1}{X_n}-\frac{1}{X_r}\ll\frac{1}{X_r}. \tag{6}$$

In Eq. (4), the second term is of second order with respect to the first, and the sixth and seventh terms are of second order with respect to the third term. We delete the second, sixth, and seventh terms and obtain

$$N(0)-N(\infty)\propto\frac{U_r}{(1+\alpha)X_r(X_r+1)}-(U_R+U_C)\left(1-\frac{1}{X_r}\right)\propto\frac{1}{1+\alpha}-\frac{U_{\rm ns}}{U},\tag{7}$$

where $U_{\rm ns}$ is the total nonresonant absorption coefficient ($U_{\rm ns}=U_R+U_C$). If the first term in Eq. (7) is less than the second term, the intensity of the backscatter γ-ray spectrum will be negative.

Equation (7) lends itself to a simple physical interpretation of negative intensities. Assume that there is a very thick absorber so that all incident γ rays are absorbed even at off-resonant Doppler velocities. As the Doppler velocity changes from off resonance to resonance, more and more γ rays that would have been absorbed nonresonantly will be absorbed resonantly. One resonantly absorbed γ ray reemits a γ ray with the probability $1/(1+\alpha)$, but if this γ ray were absorbed nonresonantly, a γ ray would be reemitted with the probability $U_{\rm ns}/U$. Since the internal conversion coefficient for ^{57}Fe is rather large, it is possible for $1/(1+\alpha)$ to be less than $U_{\rm ns}/U$. In this case, at the resonant velocity the resonant absorption processes will do more to reduce the number of γ rays available for nonresonantly scattering than to produce resonantly scattered γ rays. A negative intensity may therefore appear at the resonant velocity of a thick specimen when

$$1/(1+\alpha)<U_{\rm ns}/U.\tag{8}$$

B. Analysis of conversion x-ray backscatter Mössbauer spectra

The thickness dependence of conversion x-ray backscatter spectra has not yet been treated properly; few previous works can be found.[9] For the ^{57}Fe Mössbauer effect in the experimental geometry of Fig. 1(a), the incident radiations that must be considered are 14.4-keV recoilless γ rays, 14.4-keV nonrecoilless γ rays, and 6.4-keV x rays. Other high-energy γ rays (122 keV and 136 keV) are not included in our analysis for two reasons: (1) their nonresonant absorption coefficients are much smaller than that for 14.4 keV, and (2) the fluorescent x rays induced by them are independent of the Doppler velocity, so they are not relevant to the peak height $N(0)-N(\infty)$. (They are, however, relevant to the calculation of the percentage effect, I_f.) The x rays at the detector originate from four physical processes:

(a) Deexcitation of ^{57}Fe nuclei after resonant absorptions, i.e., the internal conversion process: $N_{rr}(V)$.

(b) Production of $K\alpha$ fluorescent x rays by recoilless incident γ rays: $N_{rf}(V)$.

(c) Production of $K\alpha$ fluorescent x rays by nonrecoilless incident γ rays: $N_{nf}(V)$.

(d) Rayleigh and Compton scattering of the incident 6.4-keV x rays: $N_{R+C}(V)$.

We make the following assumptions and definitions.

(1) The recoilless fraction of incident 14.4-keV γ rays has a single-line Lorentzian intensity distribution:

$$U(E,V)=\frac{2f_0I_0}{\pi\Gamma}\frac{(\Gamma/2)^2}{[E-(E_0+V)]^2+(\Gamma/2)^2},\tag{9}$$

where E is energy of the incident γ rays, V is equal to E_0v/c, v and c are the Doppler velocity and the speed of light, respectively, Γ is the half-width of the Lorentzian function, and E_0 is the resonant energy of the γ-ray source that has a 14.4-keV γ-ray intensity of I_0.

(2) The incident of 6.4-keV x rays have an intensity of αf_yI_0, where f_y is the x-ray fluorescent yield coefficient.

(3) The absorption of the 14.4-keV incident γ rays by the absorber is

$$U(E)=U_r(E)+U_R+U_C+U_p=U_r(E)+U_t,\tag{10}$$

where U_p is the photoelectronic absorption coefficient and $U_r(E,E_1)$ is the Lorentzian function absorption profile:

$$U_r(E)=U_r\{(\Gamma/2)^2/[(E-E_1)^2+(\Gamma/2)^2]\},\tag{11}$$

and E_1 is the mean resonant energy of the absorber.

(4) The absorption of outgoing 6.4-keV x rays is defined as U_2.

Using the model shown in Fig. 1(b) and considering the dependence of the resonant absorption on the incident γ-ray energy, we have derived the mathematical expression of the x-ray intensity for each of the four (a)–(d) processes. With the definitions $y=2(E-E_0)/\Gamma$, $S_0=2V/\Gamma$, $S_1=2(E_1-E_0)$, $T=(U_1\csc\beta_1+U_2\csc\beta_2)t_0$, the four contributions to the total conversion x-ray intensity are

$$N_{rr}(S_0)=\frac{f_0I_0U_r(\csc\beta_1)\alpha f_y}{\pi(1+\alpha)(U_1\csc\beta_1+U_2\csc\beta_2)}\times\int_{-\infty}^{\infty}dy\,Z(y,S_0),\tag{12}$$

$$N_{rf}(S_0)=\frac{f_0I_0U_pf_y\csc\beta_1}{\pi(U_1\csc\beta_1+U_2\csc\beta_2)}\times\int_{-\infty}^{\infty}dy[(y-S_1)^2+1]Z(y,S_0),\tag{13}$$

$$N_{nf}=\frac{I_0(1-f_0)U_pf_y\csc\beta_1}{U_1\csc\beta_1+U_2\csc\beta_2}[1-\exp(-T)],\tag{14}$$

$$N_{C+R}=\frac{I_0\alpha f_y(U_C+U_R)\csc\beta_1}{U_2(\csc\beta_1+\csc\beta_2)}\times\{1-\exp[-U_2t_0(\csc\beta_1+\csc\beta_2)]\},\tag{15}$$

where

$$Z(y,S_0)=\frac{1-\exp\{-T[(y-S_1)^2+x^2]/[(y-S_1)^2+1]\}}{[(y-S_0)^2+1][(y-S_1)^2+x^2]},\tag{16}$$

$$x^2=1+U_r\csc\beta_1/(U_1\csc\beta_1+U_2\csc\beta_2).\tag{17}$$

A complete derivation of these expressions is provided in Ref. 10.

C. A comparison of γ-ray and conversion x-ray backscatter Mössbauer spectra

For both γ-ray and conversion x-ray backscatter spectra, there are three kinds of scattering:

(i) recoilless incident γ rays scattered resonantly [e.g., contributions (1) and (2) of γ-ray backscatter spectra, and contribution (a) of conversion x-ray backscatter spectra],

(ii) recoilless incident γ rays scattered nonresonantly [e.g., contributions (3), (4), and (5) of γ-rays backscatter spectra, and contribution (b) of conversion x-ray backscatter spectra],

(iii) nonrecoilless incident γ rays scattered nonresonantly [e.g., contributions (6) and (7) of γ-ray backscatter spectra, and contributions (c) and (d) of conversion x-ray backscatter spectra].

The first two kinds of scattering are dependent on the Doppler velocity, while the third is not, as illustrated in Fig. 3. Notice that the nonresonant scattering of the recoilless incident γ rays shows a "dip" at resonance because off resonance all the incident recoilless γ rays are subject to nonresonant absorption and scattering, but at resonance many of the incident γ rays are absorbed resonantly.

As explained in Sec. IV A, the difference between saturation thicknesses of the resonant and nonresonant absorptions causes the nonmonotonic relationship between peak height and absorber thickness. This difference is important for both γ-ray and conversion x-ray Mössbauer spectra, so the feature of nonmonotonic saturation should occur for both backscatter spectra. Whether or not negative intensities appear at resonance depends on a competition between the fraction of γ rays emitted after resonant absorptions and the fraction of γ rays emitted after nonresonant absorptions. If the second fraction is larger than the first fraction, the intensity at resonance may be negative. For γ-ray backscatter spectra, the first fraction is $1/(1+\alpha)$, and the second fraction is U_{ns}/U. For conversion x-ray backscatter spectra, for one resonantly absorbed incident γ-ray photon the probability to produce one 6.4-keV conversion x-ray photon is $f_y\alpha/(1+\alpha)$, and for one nonresonantly absorbed incident γ-ray photon, the probability to produce one 6.4-keV fluorescent x-ray photon is $f_y\phi U_p/U$, where ϕ is the fraction of 6.4-keV $K\alpha$ photons of all fluorescent x-ray photons excited by 14.4-keV γ rays. The condition for negative intensity at resonance in conversion x-ray backscatter spectra is

$$\alpha/(1+\alpha) < \phi(U_p/U). \tag{18}$$

The differences between Eqs. (8) and (18) are interesting. The total nonresonant absorptions U include photoelectronic absorptions U_p and Rayleigh and Compton scattering absorptions U_{ns}. Both U_p and U_{ns} increase with atomic number, but U_p increases faster than U_{ns}.[11] Consequently U_{ns}/U is largest for light elements while U_p/U is largest for heavy elements. Negative intensities in γ-ray backscatter spectra are favored when the Mössbauer nucleus is embedded in a matrix of light elements, but negative intensities in conversion x-ray backscatter spectra are favored when the Mössbauer nucleus is embedded in a matrix of heavy elements.

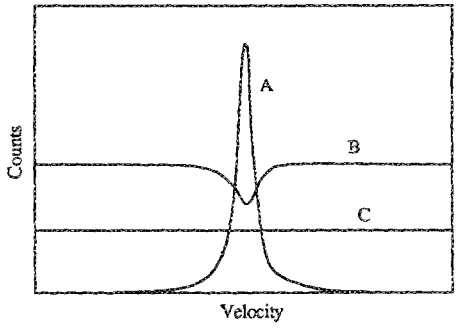

A: resonant scattering of the recoilless incident Y -rays

B: non-resonant scattering of the recoilless incident Y -rays

C: non-resonant scattering of the non-recoilless incident Y -rays

FIG. 3. Three contributions to the intensity of a backscatter Mössbauer spectrum.

III. NUMERICAL CALCULATIONS

The mathematical expressions[6] for calculating the intensities of γ-ray and conversion x-ray backscatter Mössbauer spectra as a function of absorber thickness can be solved analytically only for very thin or very thick absorbers. Where necessary, we have performed numerical calculations of the peak height of Mössbauer spectra versus specimen thickness at resonance. At resonance ($S_t = S_0$), the integrations in Eqs. (7)–(12) in Ref. 6 and Eqs. (12) and (13) in the present work become

$$\frac{1}{\pi}\int_{-\infty}^{\infty} dy\, Z(y,S_0) = \frac{2}{\pi}\int_0^{\infty} dy \frac{1-\exp[-T(y^2+x^2)/(y^2+1)]}{(y^2+1)(y^2+x^2)}, \tag{19}$$

$$\frac{1}{\pi}\int_{-\infty}^{\infty} dy[(y-S_0)^2+1]Z(y,S_0) = \frac{2}{\pi}\int_0^{\infty} dy \frac{1-\exp[-T(y^2+x^2)/(y^2+1)]}{y^2+x^2}. \tag{20}$$

At off-resonant velocities ($|S_t - S_0| \gg 0$), the integrations can be solved analytically:

$$\frac{1}{\pi}\int_{-\infty}^{\infty} dy\, Z(y,S_0) = 0, \tag{21}$$

$$\frac{1}{\pi}\int_{-\infty}^{\infty} dy[(y-S_0)^2+1]Z(y,S_0) = 1-\exp(-T). \tag{22}$$

From Eq. (22), it can be seen that the saturation thickness for the intensity at off-resonant velocities is $1/T$; from Eqs. (19) and (20), the saturation thickness for the intensity at resonance is between $1/T$ (when $y=\infty$) and $1/(Tx^2)$ (when $y=0$). Figures 2, 5(d), and 6 show the results of numerical calculations for some materials. The parameters used are listed in Table I. Nonresonant scattering of other incident radiations will modify quantitative features of the percentage effect shown in Fig. 2(b). We are least certain about the accuracy of the Rayleigh and Compton scattering coefficients.[12]

IV. EXPERIMENTS

The objectives of the experiments were (1) to test Bara's conditions for negative intensities in γ-ray backscatter spec-

TABLE I. Parameters used in the numerical calculations.

	Stainless steel (Fig. 2)	0.1 wt. % Fe in Be (Fig. 5)	Pure Fe (Fig. 6)
f_0	0.8	0.7	0.7
f_1	0.75	0.7	0.7
$U_r(\text{cm}^{-1})$	2400	0.76	870.9 (peak1)
$U_R(\text{cm}^{-1})$	26.8	0.111	6.17
$U_e(\text{cm}^{-1})$	3.8	0.254	0.77
$U(\text{cm}^{-1})$ (14.4 keV)	450	0.861	517.7
α	8.21	8.21	8.21
β_1(deg)	90	90	90
β_2(deg)	60	60	60
$U(\text{cm}^{-1})$ (6.4 keV)			520.2 580.6
$U_r(\text{cm}^{-1})$			(peak 2) 290.3
$U_r(\text{cm}^{-1})$			(peak 3)
References	7	12	12

tra, and (2) to test it conversion x-ray backscatter spectra have the nonmonotonic peak height versus thickness relation predicted by the present analysis.

All Mössbauer spectra were obtained in backscatter geometry with an Austin Science Associates S-600 constant-acceleration spectrometer. All spectra were obtained with the source and absorber at room temperature. The radiation source was ^{57}Co in Rh with the intensity of about 24 mCi. The backscatter photon detector was of toroidal geometry with high geometrical collection efficiency.[13] The incident radiation passed through the hole in the toroid, and backscattered radiations entered the detector through its large toroidal window. For good counting efficiency, the detector was filled with a mixture of 47% Kr, 47% Ar, and 6% methane gas to obtain γ-ray backscatter spectra, and with a mixture of 95% Ar and 5% methane to obtain conversion x-ray backscatter spectra. Figures 4(a) and 4(b) show the pulse height distribution from the detector for these two modes of operation. The single-channel analyzer window was set about the appropriate peak for conversion x-ray or γ-ray detection.

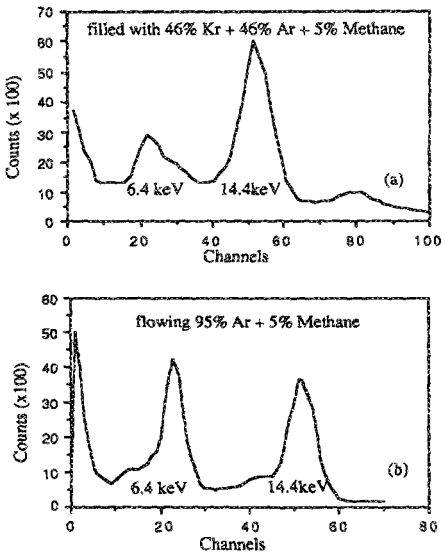

FIG. 4. Pulse height distribution of the toroidal detector for (a) γ-ray counting and (b) x-ray counting.

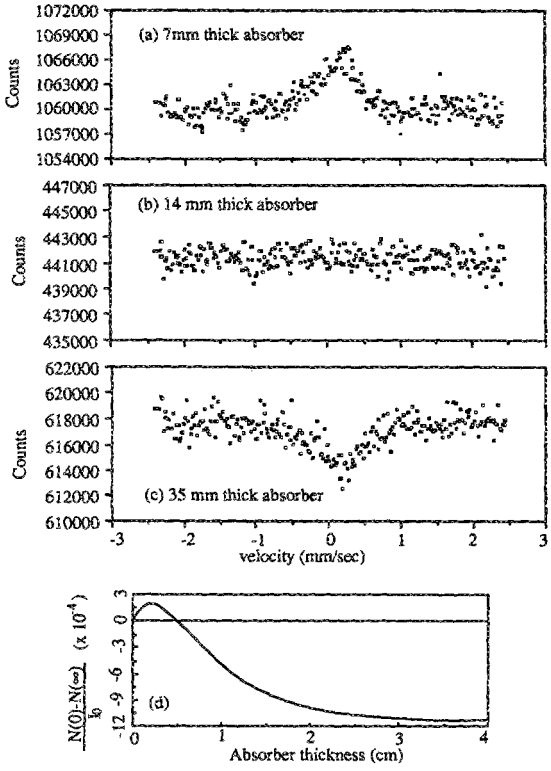

FIG. 5. Backscatter γ-ray Mössbauer spectra of Be–0.1 wt. % Fe for absorber thicknesses of (a) 7 mm, (b) 14 mm, and (c) 35 mm. (d) Numerical calculations of peak height vs absorber thickness for γ-ray backscatter Mössbauer spectrum of Be–0.1 wt. % Fe.

For the γ-ray backscatter spectra of Be-Fe, wafers of Be metal, each with a thickness of 7 mm, were stacked to obtain specimens with a series of thicknesses. The specimens had the chemical compositions 98.5 wt. % Be, 1.2% BeO, 0.060% Al, 0.1% C, 0.1% Fe, 0.08% Mg, 0.06% Si, 0.04% S, 0.04% U, and 0.04% of other elements. Three spectra from absorbers with different thicknesses are plotted in Figs. 5(a)–5(c), which show a transition from peak to dip with increasing thickness. For the conversion x-ray backscatter spectra of Fe metal, rolled iron foils of 99.999% purity were used. The foil thickness was obtained by measuring masses and areas. Foils were stacked together to make absorbers with a series of thicknesses. The peak height versus absorber thickness for peaks 1, 2, and 3 of the pure Fe sextet are plotted in Fig. 6 together with the numerical calculations for comparison.

Since all spectral intensities are proportional to the number of incident γ rays, the spectra obtained from absorbers of different thickness can be compared only when the effective collecting times for the spectra are the same. The effective collection time was defined as follows to correct the decay of the radiation source:

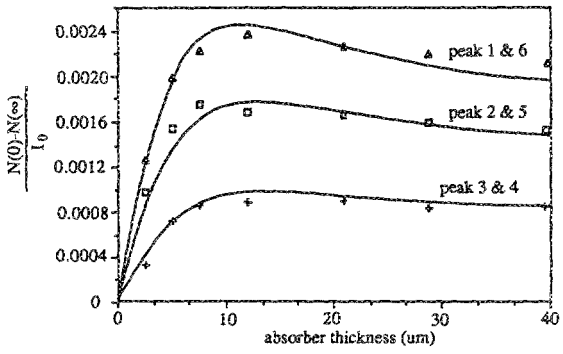

FIG. 6. The numerically calculated and experimentally measured peak height vs absorber thickness relation for conversion x-ray backscatter Mössbauer spectra of the Fe sextet.

$$I_0 \Delta t_e = \int_{t_0}^{t_0+\Delta t} I_0 \exp\left(-\frac{\ln 2}{270} t\right) dt, \tag{23}$$

where 270 days is the half-life of the ^{57}Co radioactive source, Δt and Δt_e are collecting time and effective collecting time, respectively, and t_0 is the time when a spectrum collection starts.

V. DISCUSSION

Bara's theory of the intensities of γ-ray backscatter Mössbauer spectra predicts the occurrence of a negative intensity peak that he confirmed experimentally.[8] In Figs. 5(a)–5(c), we show the change of the γ-ray Mössbauer spectrum peak intensity from positive to negative as the absorber thickness increases. The thickness of transition from positive to negative intensity is calculated from Bara's theory to be 5 mm, and the experimental thickness is 14 mm. This discrepancy may originate from one or more causes:

(1) The experimental spectra are somewhat broader than the theoretical Lorentzian width. This has the effect of reducing the recoilless cross section at resonance, and hence increasing the transition thickness.

(2) The calculated result shown in Fig. 5(d) is for the case when $\beta_1 = 90°$ and $\beta_2 = 60°$, but our detector has a toroidal shape so β_2 varies from 0° to 90°.

(3) There is an uncertainty in the accuracy of the Rayleigh and Compton scattering coefficients as explained in Sec. III. Especially for the case of dilute Fe in a matrix of light elements, these coefficients are large enough with respect to the resonant absorption coefficient so that this uncertainty could be responsible for large errors in the transition thickness.

(4) We did not obtain spectra for thicknesses between 7 and 14 mm, so the transition thickness may be in this range.

For the present theory of conversion x-ray backscatter Mössbauer spectra, the experimental data and numerical calculation show excellent agreement in how the peak height varies nonmonotonically with the thickness of the absorber (Fig. 6). In these numerical calculations the uncertainty in Rayleigh and Compton scattering coefficient is less important because thye are 1 or 2 orders smaller than the resonant absorption coefficient.

An experiment is underway to determine if negative intensities in conversion x-ray backscatter Mössbauer spectra will occur when ^{57}Fe nuclei are embedded in a matrix of heavy elements.

VI. CONCLUSIONS

We note the following.

(1) Negative intensities in γ-ray backscatter Mössbauer spectra can occur when the resonant nuclei are embedded in a matrix of light elements. For thick absorbers the condition for the occurrence of this negative intensity is

$$1/(1+\alpha) < U_{ns}/U.$$

(2) A new treatment of the intensities in conversion x-ray backscatter Mössbauer spectra that parallels Bara's theory for γ-ray backscatter spectra has been developed. As for γ-ray backscatter spectra, conversion x-ray backscatter spectra have a nonmonotonic peak height versus specimen thickness dependence. For thick absorbers the condition for the occurrence of negative intensities in conversion x-ray backscatter Mössbauer spectra is

$$\alpha/(1+\alpha) < \phi U_p/U.$$

(3) Negative peak intensities in conversion x-ray backscatter Mössbauer spectra are favored when the resonant isotope is in a matrix of heavy elements, but negative peak intensities in γ-ray backscatter Mössbauer spectra are favored when the resonant isotope is in a matrix of light elements.

ACKNOWLEDGMENT

This work is supported by the Director, Office of Energy Research, Office of Fusion Energy, Development and Technology Division of the U.S. Department of Energy, under Contract No. DE-AC03-76-SF00098.

[1]P. Debrunner and R. J. Morrison, Rev. Sci. Instrum. **36**, 145 (1965).
[2]B. Balko and G. R. Hoy, Phys. Rev. B **10**, 4523 (1974).
[3]B. Fultz and J. W. Morris, Jr., Nucl. Instrum. Methods **188**, 197 (1981); **211**, 569 (1983).
[4]J. J. Bara and B. F. Bogacz, Phys. Status Solidi A **44**, K107 (1977).
[5]J. J. Bara and B. F. Bogacz, Mössbauer Effect Ref. Data J. **3**, 217 (1981).
[6]J. J. Bara, Phys. Status Solid A **58**, 349 (1980).
[7]N. K. Jaggi, Ph.D thesis, University of Bombay, Trombay (1982).
[8]J. J. Bara, J. Phys. (Paris) Colloq. **41**, C1-13 (1980).
[9]H. K. Chow, R. F. Weise, and P. Flinn, NSEC Special Report No. NSEC-4023, Chap. 3.
[10]Z. Mei, M. Sc. thesis, University of California, Berkeley, CA (1987).
[11]C. H. Macgillavry and G. D. Rieck, Eds., *International Tables for X-ray Crystallography*, 2nd ed. (Reidel, Dordrecht, 1983), Vol. III, Chap. 3.
[12]For calculating the Rayleigh scattering coefficient we used Eq. (9) on p. 159 and Table 3.3.1 A on p. 203, *International Tables on X-ray Crystallography*, Ref. 11. For calculating the Compton scattering coefficient we used Eq. (12) on p. 249 and Table 3.4.4.2A on p. 250, *ibid.*
[13]B. Fultz, United States Patent No. 4 393 306 (12 Jul, 1983).